

Neutron dose evaluation of Elekta Linac at two energies (10 & 18 MV) by MCNP code and comparison with experimental measurements

Shagholi N¹, Nedaie H^{2*}, Sadeghi M³, Shahvar A⁴, Darestani H¹, Banaee N⁵, Mohammadi K⁶

¹Department of Engineering, Science and Research Branch, Islamic Azad University, Tehran, Iran.

²Radiotherapy Oncology Department, Cancer Research Centre, Cancer Institute, Tehran University of Medical Sciences, Tehran, Iran. Nedaieha@sina.tums.ac.ir

³Agricultural, Medical and Industrial Research School, Tehran, Iran.

⁴Agriculture medical and industrial school science and technology institute.

⁵Young Researchers and Elites Club, Science and Research Branch, Islamic Azad University, Tehran, Iran.

⁶Nuclear Engineering Department, Amirkabir Industrial University, Tehran, Iran.

ABSTRACT

Medical linear accelerators, besides the clinically high energy electron and photon beams, produce other secondary particles such as neutrons which escalate the delivered dose. In this study the neutron dose at 10 and 18MV Elekta linac was obtained by using TLD600 and TLD700 as well as Monte Carlo simulation. For neutron dose assessment in 20×20 cm² field, TLDs were calibrated at first. Gamma calibration was performed with 10 and 18 MV linac and neutron calibration was done with ²⁴¹Am-Be neutron source. For simulation, MCNPX code was used then calculated neutron dose equivalent was compared with measurement data. Neutron dose equivalent at 18 MV was measured by using TLDs on the phantom surface and depths of 1, 2, 3.3, 4, 5 and 6 cm. Neutron dose at depths of less than 3.3cm was zero and maximized at the depth of 4 cm (44.39 mSvGy⁻¹), whereas calculation resulted in the maximum of 2.32 mSvGy⁻¹ at the same depth. Neutron dose at 10 MV was measured by using TLDs on the phantom surface and depths of 1, 2, 2.5, 3.3, 4 and 5 cm. No photoneutron dose was observed at depths of less than 3.3cm and the maximum was at 4cm equal to 5.44mSvGy⁻¹, however, the calculated data showed the maximum of 0.077mSvGy⁻¹ at the same depth. The comparison between measured photo neutron dose and calculated data along the beam axis in different depths, shows that the measurement data were much more than the calculated data, so it seems that TLD600 and TLD700 pairs are not suitable dosimeters for neutron dosimetry in linac central axis due to high photon flux, whereas MCNPX Monte Carlo techniques still remain a valuable tool for photonuclear dose studies.

Indexing terms/Keywords

Neutron; TLD600; TLD700; dosimetry; Monte Carlo

Academic Discipline And Sub-Disciplines

Medical physics

SUBJECT CLASSIFICATION

Medical physics

TYPE (METHOD/APPROACH)

Experimental study of neutron dose measurements

Council for Innovative Research

Peer Review Research Publishing System

Journal: JOURNAL OF ADVANCES IN PHYSICS

Vol. 6, No.1

www.cirjap.com , japeditor@gmail.com



1. INTRODUCTION

High energy photon beams from medical linacs, besides the clinically useful electron and photon beams, produce other secondary particles such as neutrons. Neutrons are by far the most significant secondary particles in the dosimetry of treatments because of their high range in ordinary matter and high LET of their interaction products[1]. The production of photoneutrons, mainly as the result of photons interaction with high Z materials appear in the head of the accelerators [2].

The neutron dose evaluation in radiotherapy treatments is so difficult. Neutron fluence and the spectra in water have been measured using bubble detectors, superheated drop detectors [3-6], ^{197}Au -based Bonner spheres ⁽⁷⁾ and Bonner sphere with thermoluminescent dosimeters [8-9].

Thermoluminescent (TL) dosimeters are usually of interest because of having small size and their suitability for large scale measurements. In fact, thermoluminescent dosimeters (TLDs) are currently used for measuring the absorbed dose in any radiation field for either industrial or medical applications. The wide application of TLDs is due to both their small dimensions and also their tissue-equivalence; these features allow accurate measuring of the absorbed dose distribution [10-13]. The TL technique is also applied to discriminate the various radiation contributions after the exposure to photon and proton beams. As explained in the ICRU report 26 (26th report of ICRU) [14], the use of a suitable pair of dosimeters, one is more sensitive to neutrons and the other is more sensitive to photons, is needed to discriminate the contributions of gamma photons and neutrons in a mixed field. The TL dosimeters pairs usually chosen for measurements in a thermal neutrons and gamma mixed fields, are $^7\text{LiF:Mg,Ti}$ (TLD-700) and $^6\text{LiF:Mg,Ti}$ (TLD-600). TLD600 chips are chosen because they are enriched of ^6Li which has a high cross-section (about 940 barn) for the reaction with thermal neutrons ($^6\text{Li}(n,\alpha)^3\text{H}$). The high LET secondary particles (2.07MeV α -particles and 2.74MeV tritons) emitted in this reaction, release their high energy inside the dosimeter. Therefore, TLD600 dosimeters are much more sensitive to thermal neutrons than TLD700 dosimeters which are enriched of ^7Li , which interact very weakly with thermal neutrons. On the other hands, the sensitivity to gamma photons for both types of dosimeters is approximately equal because the interaction with photons depends on the atomic number (not atomic mass) of the atoms inside the dosimeter [12].

All the measurement procedures offer valuable information that can be compared with the results of Monte Carlo (MC). The MC simulation has been used to study different problems related to neutron dosimetry [15]. Kase et al. calculated neutron fluence and spectra at different positions surrounding a Varian Clinac 2100C/2300C linac[16]. Ongaro et al. studied the production of neutrons in the high-Z components of a Siemens Mevatron linac[17]. Chibani and Ma investigated the field size effects, off-axis dose profiles, neutron contribution from the linac head, dose contribution from gamma capture rays, phantom heterogeneity effects and effects of primary electron energy shift in some linac configurations[18]. Zanini et al. calculated neutron ambient dose equivalent for different collimator configurations in a Varian Clinac 2300 C/D[19]. Pena et al. studied the effects of different accelerator head modelling and room geometries on the neutron fluence and spectra for a Siemens Primus linac[1]. Recently [20], dose to patients due to the emitted photoneutrons were calculated by carrying out the simulations with Geant4[21].

In this study, the neutron contribution yielded by a medical linac has been evaluated using TL dosimeters and the Monte Carlo N Particle (MCNPX) version 2.6 [22].

2. Materials and Methods

2.1. Dosimeters

^6LiF and ^7LiF which were doped with Mg, Ti manufactured by Harshaw company were selected as thermoluminescent dosimeters for this study. These TLD600 (with 95.6% ^6LiF) and TLD700 (with 99.9% ^7LiF) are in the form of chips with size of $3 \times 3 \times 0.9\text{mm}^3$. Before irradiating, all dosimeters were annealed according to the recommendations of the manufacturer. Both kinds of TLDs have been heated at 400°C for 1 h, gradually cooled to room temperature and heated to 100°C for 2 h. TLDs have been read out at KFKI RMKI TLD reader (KFKI Research Institute of the Hungarian Academy of Sciences, Budapest Hungary). This instrument gives the TL read-out in count. The reading cycle was the same for all the samples, consisting of in a linear warming up with a rate of $11^\circ\text{C}\cdot\text{s}^{-1}$ starting from 100°C up to 300°C . The glow curve was acquired during a time of 30 s.

2.2. Neutron and gamma dose discrimination

Application of a suitable pair of dosimeters, which one is more sensitive to neutrons and the other, is more sensitive to photons is necessary to determine the values of neutronic and photonic doses in a mixed radiation field. For exposition in mixed radiation field, the response of these detectors (e.g. TLD600 and TLD700) can be related to the gamma and neutrons dose through the following equations[14].

$$\begin{cases} R_{600}^{n+\gamma} = f_{600}^n D_n + f_{600}^\gamma D_\gamma \\ R_{700}^{n+\gamma} = f_{700}^n D_n + f_{700}^\gamma D_\gamma \end{cases} \quad (1)$$



where $R_{600}^{n+\gamma}$ and $R_{700}^{n+\gamma}$ are the responses of the TLD600 and TLD700 respectively to the mixed field and f_{600}^γ , f_{600}^n are the sensitivity factors to photons and neutrons of TLD600 respectively and f_{700}^γ , f_{700}^n are the sensitivity factors to photons and neutrons of TLD700, respectively. The expressions of D_γ and D_n can be deduced through inverting these equations:

$$\begin{cases} D_\gamma = \frac{f_{700}^n R_{600}^{n+\gamma} - f_{600}^n R_{700}^{n+\gamma}}{f_{600}^\gamma f_{700}^n - f_{700}^\gamma f_{600}^n} \\ D_n = \frac{f_{600}^\gamma R_{700}^{n+\gamma} - f_{700}^\gamma R_{600}^{n+\gamma}}{f_{600}^\gamma f_{700}^n - f_{700}^\gamma f_{600}^n} \end{cases} \quad (2)$$

Since neutron sensitivity of TLD600 is about 10^3 times of TLD700 ⁽²³⁾, we assumed $f_{700}^n = 0$. This allows deriving the gamma and thermal neutron dose with the following simplified equation:

$$\begin{cases} D_\gamma = \frac{R_{700}^{n+\gamma}}{f_{700}^\gamma} \\ D_n = \frac{f_{700}^\gamma R_{600}^{n+\gamma} - f_{600}^\gamma R_{700}^{n+\gamma}}{f_{700}^\gamma f_{600}^n} \end{cases} \quad (3)$$

To obtain the gamma and neutron doses, the user must know the sensitivity factor of gamma and neutron components for each TLDs.

To know these sensitivity factors the gamma and neutron calibrations of the TLDs were performed. Gamma calibration was done in two procedures; by 10 and 18 MV photon beams. Neutron calibration was performed by ²⁴¹Am-Be source.

2.3. TLD calibration

2.3.1. TLD personal calibration

Each TLD chip an ECC (Element Correction Coefficient), correcting its sensitivity to a definite dose. An ECC is generally determined by irradiating a group of TLDs to a known dose level and referring the response to the average TL value. Calculating the ECC is performed using equation (4), where TLR is the average read-out of the TLDs, and TLR_j is the read-out of the TLD number j . This ensures that the entire population of TLDs respond almost the same [24].

$$ECC_j = \frac{\langle TLR \rangle}{TLR_j} \quad (4)$$

To measure the ECC of each TLD, TLDs were exposed to the same dose of 430 mGy of ⁶⁰Co gamma source.

2.3.2. Gamma and neutron calibration

The following function as gamma sensitivity curve for TLD600 and TLD700 was used:

$$I_\gamma = f^\gamma D_\gamma \quad (5)$$

Where I_γ is the TL read-out or the TL intensity (area under glow curve) and f^γ is the TLD gamma sensitivity factor. The sensitivity factor is the reverse of the calibration factor, ($f^\gamma = \frac{1}{\alpha_\gamma}$).

Since TLD response is energy dependent, it is better to calibrate the dosimeters by the energy which is used in experiment [25]. Therefore, gamma calibration was performed by 10 and 18 MV photon beams.

To do the calibration by 10 and 18 MV photon beams, irradiation was done in two procedures; by a thin layer of Cadmium (Cd) over TLDs and without it. Cd is used to absorb thermal neutrons. By Cd and irradiating pairs of TLDs to a same dose, the ratio of sensitivity factors is achieved through equations (1). TLD700 sensitivity factor is measured separately by its irradiation to several definite doses of 10 and 18MV linac. Conclusively, TLD600 sensitivity factor is also obtained.

The gamma irradiation of TLD chips by linac were performed in a Plexiglas phantom $30 \times 30 \times 30 \text{ cm}^3$, with a field size of $20 \times 20 \text{ cm}^2$, at depth of 2.5cm (d_{max} at 10MV) and 3.3 cm (d_{max} at 18MV) and the SSD of 100 cm. Pairs of TLDs with a thin layer of Cd over them, were exposed to definite doses of 0.5, 1 and 1.5Gy at depth of d_{max} . TLD700 chips were also separately exposed to definite doses of 0.5, 1, 1.5 and 2Gy at depth of d_{max} .

For neutron calibration, $^{241}\text{Am-Be}$ source with the activity of 5Ci was applied. All dosimeters were located at 1m distance from the source, behind 6cm polyethylene as a moderator. The dose rate at the point of TLDs was measured $131.4\mu\text{Sv/h}$. Neutron irradiations were done in four different time intervals; 21, 44, 64.3 and 111.3h equal to 2.76, 5.78, 8.45 and 14.62mSv.

The experimental data was analyzed through the following linear equation:

$$I_n = f^n D_n \quad (6)$$

Where D_n represents the neutron dose value and f^n is the sensitivity of TLD600 to neutron and I_n shows the net signal of TLDs (the difference between TLD600 and TLD700 responses).

2.4. Irradiation

Dosimeters were put in the dedicated holes on $30 \times 30 \times 15\text{cm}^3$ Plexiglas slab phantoms, with a field size of $20 \times 20\text{cm}^2$ and source-detector distance of 100 cm. Linac was set to deliver 3Gy at the point of 3.3cm depth (D_{max}).

Measurements were performed at central axis by six pairs of TLD600 and TLD700 on the phantom surface and depths of 1, 2, 2.5, 3.3, 4 and 5 cm for 10MV and on the phantom surface and depths of 1, 2, 3.3, 4, 5 and 6 cm for the energy of 18MV. In order to avoid superimposing of TLDs, each point was irradiated separately (Figure 1).

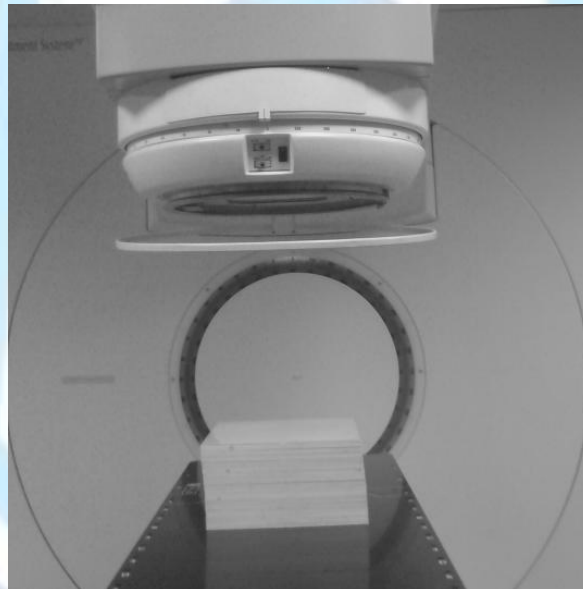


Fig. 1) Setup of experiment for irradiation of TLDs (SSD=100 cm and field size= $20 \times 20\text{cm}^2$)

2.5. Monte Carlo simulation

To assess the neutron contributions to the absorbed dose, MC simulation was used. For this purpose detailed knowledge of the geometry of the linac head (including target, ion chamber, collimators and flattening filter) is necessary. In this work, Elekta Precise linac operated at 10 and 18 MV have been studied. The geometries were modeled according to the specifications of the respective manufacturer. A cubic water phantom also simulated which its surface was at 100 cm from the source (SSD=100cm).

The first step of the simulations was to fix the characteristics of the electron beams impinging the target in linac. We assumed a point-like source emitting electrons in a single direction. The tuning was carried out by assuming that initial electrons followed a Gaussian energy distribution and fixing the maximum energy and FWHM values of this Gaussian (table 1). In these simulations, the jaws were fixed to define a field of $20 \times 20\text{cm}^2$ at the surface of the phantom, which was situated at 100 cm from the source. The neutron flux was determined in the phantom as a function of the depth, using the F4 tally. For comparison between experimental and simulation results, flux to equivalent dose conversion factor were used in the range of thermal neutron energies [22].

Table 1) Characteristics of electron Gaussian energy distribution at 10 and 18 MV beam energies (According to the specifications of the respective manufacturer)

Nominal X-RAY Beam Energy (MV)	Typical Energy and Spot size Characteristics of Electron Beam on Target			
	Peak Energy (MeV)	FWHM (MeV)	Energy Window (MeV)	FWHM (mm)
10	10.5	0.3	±0.9	1
18	15.3	0.5	±1.4	0.75

3. Results

3.1. Measurement results

Table (2) reports the gamma calibration factors of dosimeters measured by 10 and 18 MV photon beams. As it can be noted from this table, the sensitivities of TLD600 and TLD700 to gamma photons are almost the same as expected.

Table 2): TLDs Gamma calibration factor measured by 10 and 18 photon beams

Energy	Calibration factor	
	$\alpha'_{600}(\text{mGy/TL})$	$\alpha'_{700}(\text{mGy/TL})$
Linac(18MV)	$0.078 \pm 3.39\text{E-}3$	$0.089 \pm 9.44\text{E-}5$
Linac(10MV)	$0.072 \pm 2.4\text{E-}3$	$0.080 \pm 1.3\text{E-}4$

Figure (2) shows the neutron calibration curve for the TLD600 base on net TLD's response in terms of thermal neutron equivalent dose in irradiation by ²⁴¹Am-Be.

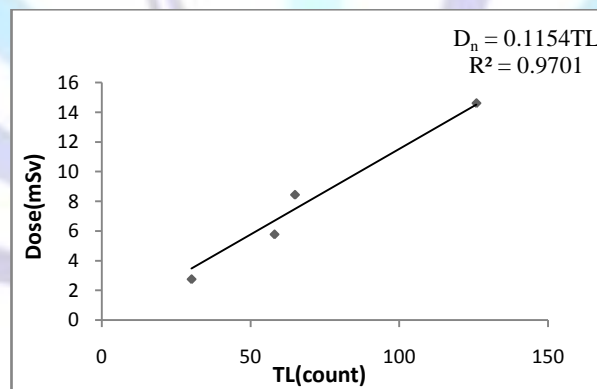


Fig. 2) TLD600 neutron calibration curve measured by Am-Be source.

TLD600 neutron sensitivity factor, f_{600}^n , and neutron calibration factor, α_{600}^n , are calculated as follows:

$$f_{600}^n = 8.6655 \left(\frac{TL}{mSv} \right)$$

$$\alpha_{600}^n = 0.1154 \left(\frac{mSv}{TL} \right)$$

Tables (3) and (4) show the photon absorbed dose and neutron dose equivalent values in central axis calculated by equations (3). Differences are also estimated by the results obtained by the ion chamber detector for gamma dose.



Table 3): Calculated photon absorbed dose and neutron dose equivalent values and differences for photon dose by the results obtained by the ion chamber dosimeter at 10MV

d(cm)	D _γ (mGy)	D _n (mSv/Gy)	Difference (%)
0	1328.07±40.60	0±26.78	5.8
1	2606.68±38.32	0±20.28	4.7
2	2813.45±67.76	0±37.26	6.2
2.5	2818.11±48.71	0±30.78	5.2
3.3	2826.47±42.59	3.121±43.49	2.6
4	2727.53±65.15	5.448±40.55	4
5	2641.3±47.66	4.67±23.94	3.3

Table 4): Calculated photon absorbed dose and neutron dose equivalent values and differences for photon dose by the results obtained by the ion chamber dosimeter at 18MV

d(cm)	D _γ (mGy)	D _n (mSv/Gy)	Difference (%)
0	1256.02±32.28	0±26.4	3.62
1	2647.41±77.49	0±40.8	5.55
2	3139.46±69.12	0±25.45	5.25
3.3	3077.26±115.34	14.61±53.95	2.58
4	2916.39±102.4	44.39±55.85	1.09
5	2827.91±81.22	42.25±43.53	0.99
6	2681.11±46.55	36.62±33.01	2.58

3.2. Monte Carlo results

Figures (3) and (4) indicate the comparison between experimental PDD measured by Ion chamber (solid curves) and calculated PDDs (dots). The maximum difference is less than 3% which is showing good agreement between experimental measurements and simulation.

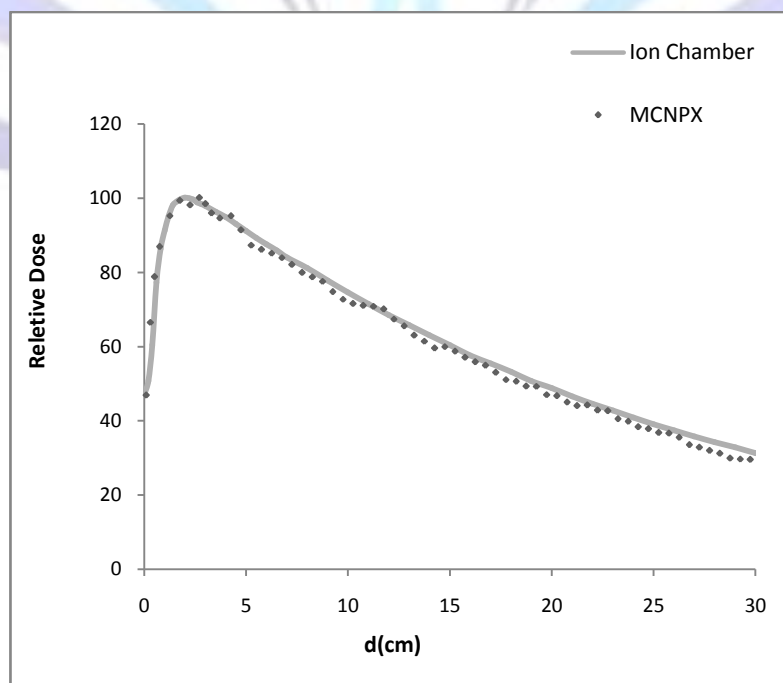


Fig. 3) Comparison between measured and calculated PDDs for 20 × 20 field size at 10MV

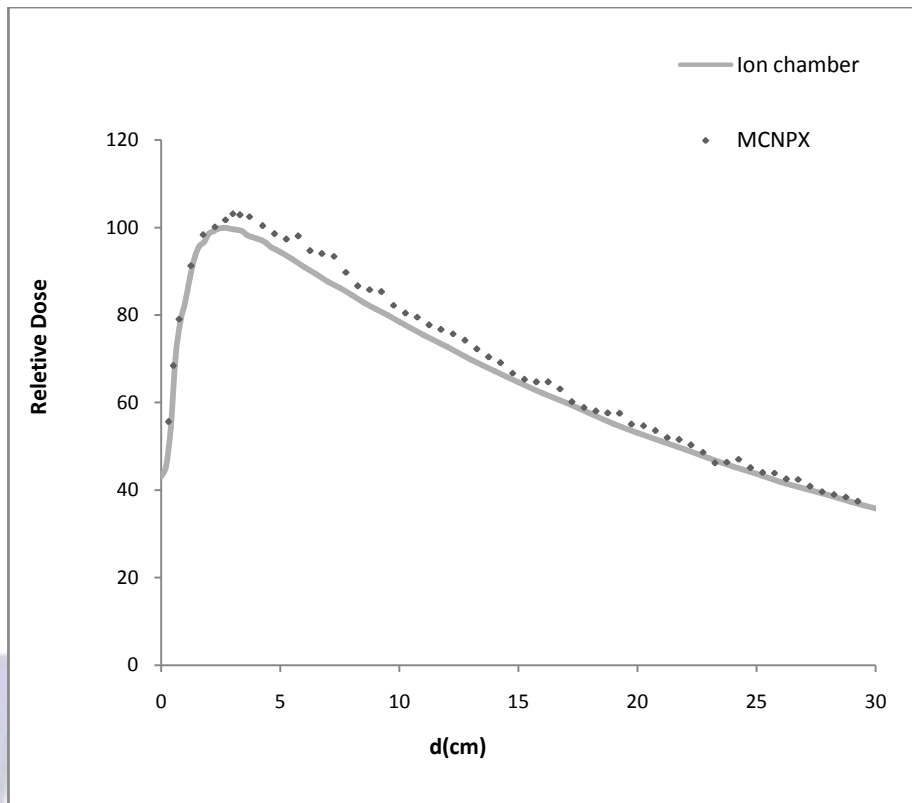


Fig. 4) Comparison between measured and the calculated PDDs for 20 × 20 field size at 18MV

One of the most important issues in this type of calculations is related to the neutron dose equivalent, H, which a patient can receive in a radiotherapy treatment. Figure (5) shows the obtained results, along the beam axis, as a function of the depth in the phantom.

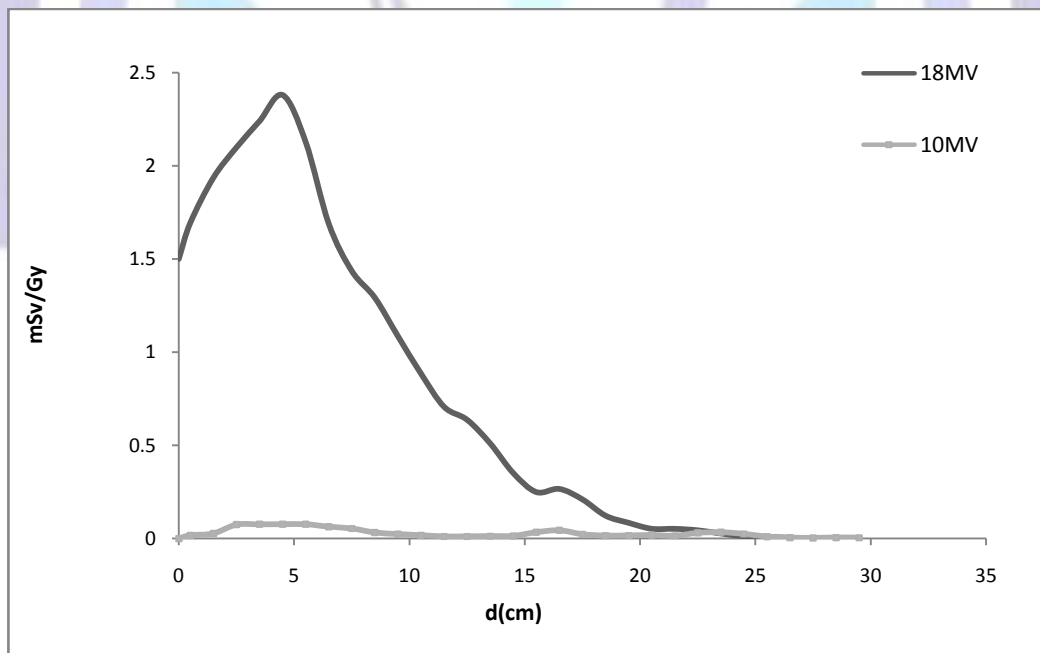


Fig. 5) Thermal neutron dose equivalent calculated, H, as a function of depth in the phantom, along the beam axis



4. Discussion

Several studies[3-9,15-21]have been performed to evaluate the photoneutron dose to the patients. However, no similar work has been carried out by TLD pairs along the beam axis, in them.

The comparison of measured and calculated data of neutron equivalent dose at the corresponding measured depths is shown in table (5).

Table 5) Comparison between measured and calculated neutron equivalent dose at 10 and 18MV

d(cm)	D_n (mSv)measurement		D_n (mSv)calculation	
	18MV	10MV	18MV	10MV
0	0	0	0.9	0
1	0	0	1.69	0.022
2	0	0	2.12	0.051
2.5	-	0	-	0.075
3.3	14.61	3.12	2.09	0.076
4	44.39	5.44	2.23	0.077
5	42.25	4.67	2.32	0.077
6	36.62	-	2.1	-

As it can be noted in this table, the measured neutron equivalent dose is much more than calculated data since the measured data are 55 and 15 times more than 10 and 18MV calculated data respectively. These large differences can be due to high TLD error for neutron dosimetry in neutron-gamma mixed field of linac with high photon flux. Our results are in agreement with Triolo's study [26] who did the neutron and gamma dosimetry with TLD600 and 700, in neutron-gamma mixed field with high photon flux (like medical accelerator) and with high neutron flux (like reactor), they showed high error in gamma and neutron measurement. Esposito's study [27] also reported TLD's high error in neutron dosimetry in linac field.

The comparison between two energies indicates that the measured neutron dose at 18MV in average is 8 times more than 10 MV. On the other hand, consideration of calculated data at two energies illustrates that the neutron equivalent dose at the energy of 18 MV in average is 40 times more than the other one. This result is due to the probability of photonuclear interactions and neutron production which occurred with the linac head components, while this probability is decreased for low energies like 10MV.

As it can be seen in Figure (5), the dose variation and the region of maximum neutron dose points are about the same for two energies. The maximum value at the energy of 10MV is in the range of depths 2.5-5.5cm (0.077mSvGy^{-1}) and the peak of the 18MVcurve is at the depth of 4.5cm (2.37mSvGy^{-1}). These maximum dose values at primary depths indicate that the most of the neutrons were produced in the linac head were thermalized at these points. The maximum value of calculated equivalent neutron dose at the energy of 18MV in Martínez-Ovalle's study [15] was at the phantom surface (2.5mSvGy^{-1}) and then the neutron dose decreased. Variation of neutron dose against the phantom depth except initial points in our work is in a good agreement with Martínez-Ovalle's study. The difference between the maximum point locations is due to that Martínez-Ovalle's calculations were included any types of neutron such as fast and thermal. The range of calculated neutron equivalent dose which obtained by Verhaegen and Seuntjens[28] by 18MV photon beams energy ($2-5\text{mSvGy}^{-1}$) is a bit more than that of ours results, in this work the neutron equivalent dose is calculated in general and there is no distinction between thermal and fast neutrons since in our study only the thermal neutrons were taken into account.

Similar works were carried out by M. K. Saeed [20] which calculated the neutron ambient dose equivalent at the X-ray mode of 10MV equal to 0.06mSvGy^{-1} . J. C. Rivera et al. [29] also measured the neutron ambient dose equivalent by BD-PND (Bubble detector personal neutron dosimeter) at 10MV, about 0.44mSvGy^{-1} . In M. K. Saeed's study, calculations were performed for Varian linac and only the fast neutrons were taken in to account and J. C. Rivera measured the neutron dose in general for Clinac.

5. Conclusion

By observing the high discrepancies between measured and calculated results, it seems that TLD600 and TLD700 pairs are not suitable dosimeters for neutron measurement in central axis due to high photon flux, whereas MC method is a valuable tool for photonuclear dose studies.

The results of MC indicates that the equivalent neutron dose from photoneutrons to the patients in a typical linac treatment facility at the energy of 10MV is insignificant and it can be neglected while the results for 18MV is considerable and must



be taken into account because the probability of secondary cancers due to additional neutron doses will increase and is not negligible. So in a typical linac treatment facility at high energy, neutron field evaluation is necessary to optimise the treatment.

References

1. Pena, J., Franco, L., Gómez, F., Iglesias A., Pardo, J. and Pombar, M. Monte Carlo study of Siemens PRIMUS photoneutron production. *Phys. Med. Biol.* 50, 5921–5933 (2005)
2. Ma, A., Awotwi-Pratt, J., Alghamdi, A., Alfuraih, A. and Spyrou, N. M. J. Monte Carlo study of photoneutron production in the Varian Clinac 2100C linac. *Radioanalyt. Nucl. Chem.* 276, 119–123 (2008).
3. Lin, J. P., Liu, W. C. and Lin, C. C. Investigation of photoneutron dose equivalent from high-energy photons in radiotherapy. *Appl. Radiat. Isotop.* 65, 599–604 (2007).
4. D'Errico, F., Nath, R., Silvano, G. and Tana, L. In vivo neutron dosimetry during high-energy bremsstrahlung radiotherapy. *Int. J. Radiat. Oncol. Biol. Phys.* 41, 1185–1192 (1998).
5. D'Errico, F., Nath, R., Tana, L., Curzio, G. and Alberts, W. G. In-phantom dosimetry and spectrometry of photoneutrons from an 18 MV linear accelerator. *Med. Phys.* 25, 1717–1724 (1998).
6. D'Errico, F., Luszik-Bhadra, M., Nath, R., Siebert, B. R. L. and Wolf, U. Depth dose-equivalent and effective energies of photoneutrons generated by 6-18 MV X Ray beams for radiotherapy. *Health Phys.* 80, 4–11 (2001).
7. Howell, R. M., Hertel, N. E., Wang, Z., Hutchinson, J. and Fullerton, G. D. Calculation of effective dose from measurements of secondary neutron spectra and scattered photon dose from dynamic MLC IMRT for 6 MV, 15 MV, and 18 MV beam energies. *Med. Phys.* 33, 360–368 (2006).
8. Harrison, R. M., Wilkinson, M., Shemilt, A., Rawlings, D. J., Moore, M. and Lecomber, A. R. Organ doses from prostate radiotherapy and associated concomitant exposures. *Brit. J. Radiol.* 79, 487–496 (2006).
9. Reft, C. S., Runkel-Mueller, R. and Myrianthopoulos, L. In vivo and phantom measurements of the secondary photon and neutron doses for prostate patients undergoing 18 MV IMRT. *Med. Phys.* 33, 3734–3742 (2006).
10. Jungner, H., Aschan, C., Toivonen, M., Chernov, V., Toivonen, A., The abilities of LiF thermoluminescent detectors for dosimetry at boron neutron capture therapy beams, *Radiat. Meas.* 29, 3–4 (1998) 373.
11. Gambarini, G., Sinha Roy, M. Dependence of TLD thermoluminescence yield on absorbed dose in a thermal neutron field, *Appl. Radiat. Isot.* 48, 10–12 (1997) 1467.
12. Vana, N., Shöner, W., Fugger, M. The LET dependence of LiF:Mg,Ti dosimeters and its application for measurements in mixed radiation fields, *Radiat. Prot. Dosim.* 85 (1999) 263.
13. German, U., Weinstein, M., Alfassi, Z.B. On neutron–gamma mixed field dosimetry with LiF:Mg,Ti at radiation protection dose levels, *Radiat. Prot. Dosim.* 119 (2006) 314. (1979) 79.
14. ICRU. Report 26 neutron dosimetry for biology and medicine. Technical report, International Commission on Radiation Units and measurement, 1977.
15. Martínez-Ovalle, S. A., Barquero, R., Gómez-Ros, J.M. and Lallena, A. M. Neutron dose equivalent and neutron spectra in tissue for clinical Linacs operating at 15, 18 and 20 MV. *Radiation Protection Dosimetry*, pp. 1–14 (January 12, 2011).
16. Kase, K. R., Mao, X. S., Nelson, W. R., Liu, J. C., Kleck, J. H. and Elsalim, M. Neutron fluence and energy spectra around the Varian Clinac 2100C/2300C medical accelerator. *Health Phys.* 74, 38–47 (1998).
17. Ongaro, C., Nastasi, U. and Zanini, A. Monte Carlo simulation of the photo-neutron production in the high-Z components of radiotherapy linear accelerators. *Monte Carlo Methods Appl.* 5, 69–79 (1999).
18. Chibani, O. and Ma, C.-M. C. Photonuclear dose calculations for high-energy photon beams from Siemens and Varian linacs. *Med. Phys.* 30, 1990–2000 (2003).
19. Zanini, A. et al. Monte Carlo simulation of the photoneutron field in linac radiotherapy treatments with different collimation systems. *Phys. Med. Biol.* 49, 571–582 (2004).
20. Saeed, M. K., Moustafa, O., Yasin, O. A., Tuniz, C. and Habbani, F. I. Doses to patients from photoneutrons emitted in a medical linear accelerator. *Radiat. Prot. Dosim.* 133, 130–135 (2009).
21. Agostinelli, S. et al. Geant4-a simulation toolkit. *Nucl. Inst. Meth. Phys. Res. Sect. A* 506, 250–303 (2003).
22. Monte Carlo Team. MCNP5/MCNPX-exe Package, Monte Carlo N-Particle eXtended” Los Alamos National Laboratory Report; 2008. Available from: <https://mcnp.lanl.gov/> (with proper license to the author C. Tenreiro)
23. Bedogni, R., Esposito, A., Angelone, M., Chiti, M. Determination of the response to photons and thermal neutrons of new LiF based TL materials for radiation protection purposes. *IEEE Trans Nucl Sci.* 53, 1367–1370 (2006).



24. Delzer JA, Hawley JR, Romanyukha A, et al. Long-term fade study of the DT-702 LiF: Mg,Cu,P TLD. *Radiat Prot Dosim.* 131, 279–286(2008).
25. Furetta C. *Handbook of thermoluminescence.* Published by World Scientific Publishing Co. Pte, Ltd, (2003).
26. Triolo, A., Marrale, M., Brai, M. Neutron–gamma mixed field measurements by means of MCP–TLD600 dosimeter pair. *Nucl. Instr. Meth. In Phys. Res.* 183-188 (2007).
27. Esposito A., Bedogni R., Lembo L., Morelli M. Determination of the neutron spectra around an 18MV medical LINAC with a passive Bonner sphere spectrometer based on gold foils and TLD pairs. *Radiation Measurements* 43,1038 – 1043(2008).
28. Verhagen, F., Das, IJ. and Palmans, H. Monte Carlo dosimetry study of a 6 MV stereotactic radiosurgery unit. *Phys. Med. Biol.* 43, 2755-2768. printed in UK(1998).
29. Rivera, J. C., Falca, R. C. and deAlmeida, C. E. The measurement of photoneutron dose in the vicinity of clinical linear accelerators. *Radiation Protection Dosimetry*, Vol. 130, No. 4, pp. 403–409(2008).

